Ca^{2+} sparks and Ca^{2+} waves in saponin-permeabilized rat ventricular myocytes

Valeriy Lukyanenko and Sandor Györke

Department of Physiology, Texas Tech University Health Sciences Center, Lubbock, TX 79430, USA

(Received 30 April 1999; accepted after revision 28 September 1999)

1. We carried out confocal Ca^{2+} imaging in myocytes permeabilized with saponin in 'internal' solutions containing: MgATP, EGTA and fluo-3 potassium salt.

2. Permeabilized myocytes exhibited spontaneous Ca^{2+} sparks and waves similar to those observed in intact myocytes loaded with fluo-3 AM.

3. In the presence of 'low' [EGTA] (0·05 mM), Ca^{2+} waves arose regularly, even at relatively low $[Ca^{2+}]$ (50–100 nM, free). Increasing [EGTA] resulted in decreased frequency and propagation velocity of Ca^{2+} waves. Propagating waves were completely abolished at [EGTA] > 0·3 mM.

4. The frequency of sparks increased as a function of $[Ca^{2+}]$ (50–400 nM range) with no sign of a high affinity Ca^{2+}-dependent inactivation process.

5. The rate of occurrence of Ca^{2+} sparks was increased by calmodulin and cyclic adenosine diphosphate-ribose (cADPR).

In the mammalian heart, Ca^{2+} influx through voltage-dependent Ca^{2+} channels in the sarcolemma triggers Ca^{2+}-induced Ca^{2+} release from the sarcoplasmic reticulum (SR; Bers, 1991; Stern & Lakatta, 1992; Eisner *et al.* 1998). Under various conditions that result in increased cellular Ca^{2+} content Ca^{2+} release can occur spontaneously in the form of regenerative Ca^{2+} waves (Kort *et al.* 1985; Wier *et al.* 1987; Takamatsu & Wier, 1990; Lipp & Niggli, 1994; Trafford *et al.* 1995; Engel *et al.* 1995; Wussling & Salz, 1996; Cheng *et al.* 1996; Lukyanenko *et al.* 1996, 1999). Spontaneous Ca^{2+} waves have been implicated in certain cardiac dysfunctions such as triggered arrhythmias (Lakatta, 1992; Ishide, 1996). Nevertheless, the mechanisms of generation of Ca^{2+} waves and their relationship to the Ca^{2+} release process during normal excitation–contraction (E–C) coupling are not precisely understood. Recent studies using confocal Ca^{2+} imaging revealed that Ca^{2+} release during both normal E–C coupling and Ca^{2+} waves is a result of the summation of elementary release events, Ca^{2+} sparks (Cannell *et al.* 1994; Lopez-Lopez *et al.* 1995; Cheng *et al.* 1996). Ca^{2+} sparks can arise spontaneously and in response to electrical stimulation of the cell. Under normal cellular Ca^{2+} loading conditions sparks remain localized. When the cellular Ca^{2+} content is elevated they give rise to propagating Ca^{2+} waves (Cheng *et al.* 1996; Lukyanenko *et al.* 1996, 1999). The factors which could potentially influence the activity of individual Ca^{2+} release sites as well as the interaction between adjacent sites include Ca^{2+} levels in both cytosolic and SR luminal compartments, intracellular Ca^{2+} buffering, Ca^{2+} activation and inactivation properties of the release channels, and the presence of intracellular modulatory agents.

Permeabilization that allows rapid equilibration of various substances between extracellular fluid and cytosol has been a valuable tool for studying E–C coupling in both skeletal and cardiac muscle cells. In particular, Fabiato, by measuring force and aequorin light signals in permeabilized cardiac myocytes, has defined the Ca^{2+} dependence of SR Ca^{2+} release activation and inactivation (Fabiato, 1985), laying the foundation of the theory of Ca^{2+}-induced Ca^{2+} release. In the present study we used confocal Ca^{2+} imaging to explore local Ca^{2+} signalling in permeabilized cardiac cells. We investigated the role of such factors as Ca^{2+} buffering, $[Ca^{2+}]_i$ as well as calmodulin and cADPR in the modulation of local release events (Ca^{2+} sparks) and propagating Ca^{2+} waves.

METHODS

Cell isolation, permeabilization and experimental solutions

Adult Sprague–Dawley rats (200–300 g) were killed by lethal injection of Nembutal (Abbott Laboratories, 100 mg kg^{-1}, I.P.), and single ventricular myocytes were obtained by enzymatic dissociation as described previously (Györke *et al.* 1997). The cells were loaded with fluo-3 by a 20 min incubation with 5 μM fluo-3 AM (acetoxymethyl ester form, Molecular Probes) at room temperature. The Tyrode solution contained (mM): 140 NaCl, 5·4 KCl, 0·5 $MgCl_2$, 1–5 $CaCl_2$, 10 Hepes, 0·25 NaH_2PO_4, 5·6 glucose; pH 7·3. The cardiac myocytes were permeabilized with saponin (0·01 % for 45–60 s) in an 'internal' solution containing (mM): 120 potassium aspartate, 3 MgATP (free $[Mg^{2+}] \sim 1$ mM), 0·1 EGTA,

10 phosphocreatine, 5 U ml^{-1} creatine phosphokinase, and 8% dextran (40 000, to prevent osmotic swelling of the cells); pH 7·2. The control experimental solution contained (mM): 120 potassium aspartate, 3 MgATP, 0·5 EGTA, 0·114 $CaCl_2$ (free [Ca^{2+}] ~ 100 nM), 10 phosphocreatine, 0·03 fluo-3 potassium salt (TefLabs, Austin, TX, USA) and 5 U ml^{-1} creatine phosphokinase; pH 7·2. Solutions with different buffering strengths and free [Ca^{2+}] were prepared by adding appropriate amounts of K_2EGTA and $CaCal_2$. The free [Ca^{2+}] at given total Ca^{2+}, Mg^{2+}, ATP and EGTA concentrations was calculated using a computer program (WinMAXC 1.80, Stanford University, CA, USA) and verified by measurements with a spectrofluorometer D-Scan (PTI, Monmouth Junction, NJ, USA) and the Ca^{2+} indicator fura-2 (TefLabs, Austin, TX, USA). The drugs were applied through a gravity-driven perfusion system. All experiments were performed at room temperature (21–23 °C). All chemicals except fluo-3 and fura-2 were from Sigma.

Confocal microscope

Experiments were performed as described previously (Györke *et al.* 1997), using an Olympus laser scanning confocal microscope (LSM-GB200) equipped with an Olympus ×60, 1·4 NA objective. Fluo-3 was excited by light at 488 nm using a 25 mW argon laser with intensity attenuated to 1–3%. Fluo-3 fluorescence was measured at wavelengths of >515 nm. Images were acquired in the line-scan mode of the microscope at a rate of 2·1 or 8·3 ms per scan, with the scan line oriented along the longitudinal axis of the cell. An analog recording of fluorescence intensity was digitized into 640 pixels, giving a nominal pixel dimension of 0·41 μm. To reduce cell damage by the laser illumination, the position of the line scan was changed after acquiring three to six images from each particular location. Thus, in a typical cell the measurements could be performed for 10–15 min without significant alterations in Ca^{2+} spark properties.

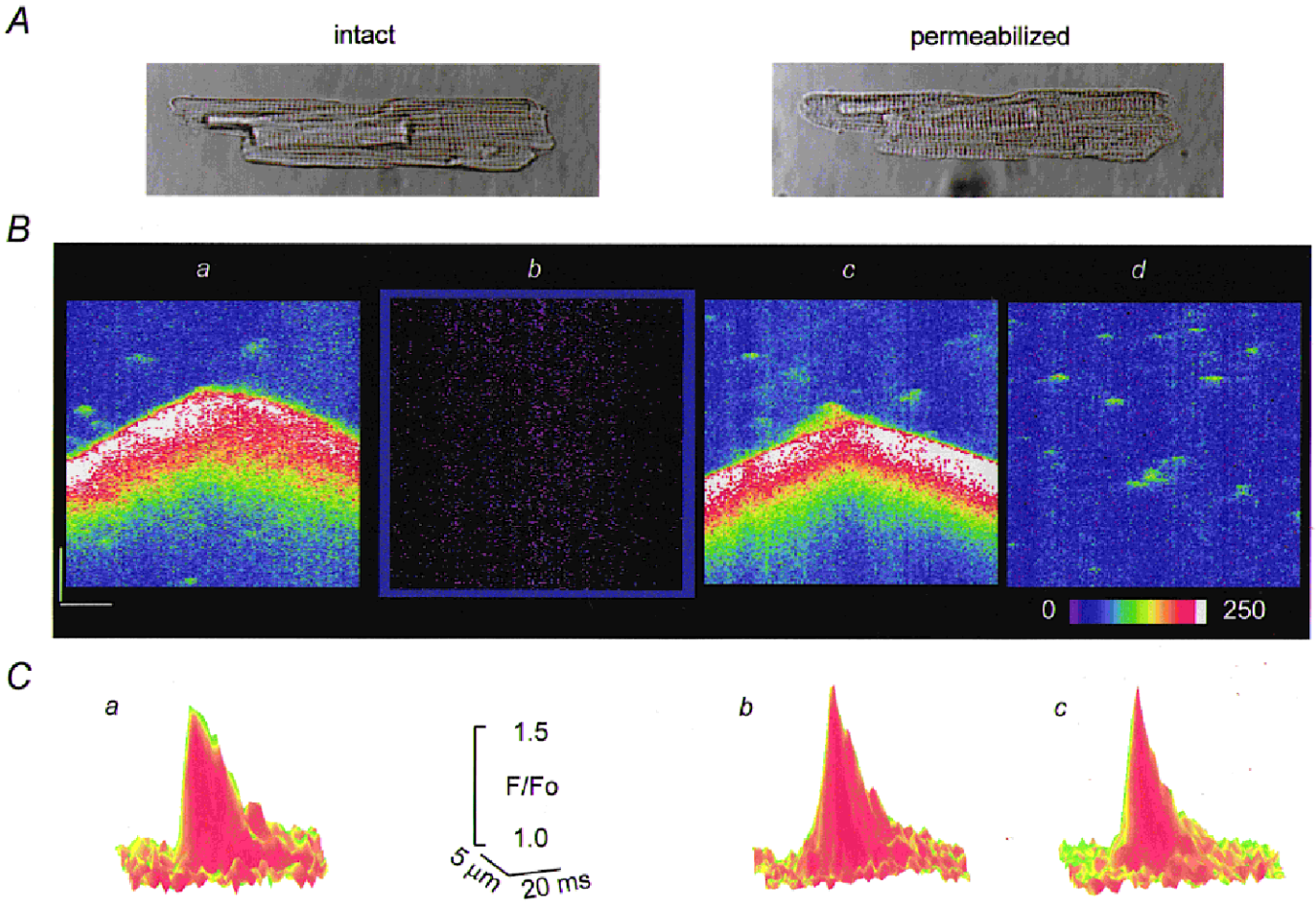

Figure 1. The effects of permeabilization on Ca^{2+} sparks and Ca^{2+} waves in ventricular myocytes

A, images of a cardiac myocyte obtained in transmitted light before and after permeabilization with saponin. *B*, line-scan images of fluorescence in a portion of the same cell pre-loaded with fluo-3 AM measured before permeabilization (*a*, $[Ca^{2+}]_o = 5$ mM), after permeabilization in an internal solution with no dye (*b*) and after addition to the internal solution 30 μM fluo-3 potassium salt in the presence of 0·1 (*c*) or 0·5 mM EGTA (*d*) (pCa 7). Calibration bars: horizontal 10 μm, vertical 0·4 s, the colour bar represents changes in units of absolute fluorescence. *C*, surface plots of Ca^{2+} sparks measured before permeabilization (*a*) and after permeabilization in the presence of 0·1 or 0·5 mM EGTA (*b* and *c*, respectively). Each plot was obtained by averaging 10 individual events.

Ca^{2+} sparks were detected and measured using a computer algorithm similar to that described previously (Song *et al.* 1997; Cheng *et al.* 1999). The program defines Ca^{2+} sparks as regions of elevated fluorescence relative to the standard deviation (S.D.) of background noise of the fluorescence image. The performance of the program at different event detection threshold settings was tested by using standard Ca^{2+} sparks of various intensities contaminated with appropriate amounts of random noise (Song *et al.* 1997). With the detection threshold set at a level of 2·6 × S.D., the amplitude of events detected with 50 % efficiency was about $1{\cdot}3F/F_o$ (where F is the recorded fluorescence intensity and F_o is background fluorescence) while the probability of false events was 1–2 %. The average propagation velocity of Ca^{2+} waves was determined by fitting a linear function to the position of the wave (defined at half-maximal amplitude) in the x–t plane (Lukyanenko *et al.* 1999). Image processing and analysis were performed using NIH Image (NIH, Bethesda, MD, USA) and IDL software (Research Systems Inc., Boulder, CO, USA).

RESULTS

Effects of permeabilization

Figure 1 illustrates the main steps of a permeabilization experiment in a single isolated rat ventricular myocyte pre-loaded with fluo-3 AM. The series of line-scan images in *B* were acquired before permeabilization (*a*), after permeabilization with 0·01 % saponin for 1 min in an internal solution containing no dye (*b*) and after addition to the internal solution of 30 μM fluo-3 potassium salt in the presence of 0·1 mM (*c*) or 0·5 mM EGTA (*d*). Photographic wide field images of the myocyte before and after permeabilization are illustrated at the top (*A*). As described previously (Cheng *et al.* 1993, 1996; Lukyanenko *et al.* 1996), the intact cell spontaneously exhibited sporadic Ca^{2+} sparks and occasional Ca^{2+} waves. Permeabilization was confirmed by the disappearance of all the fluorescence signals in the bathing solution containing no dye and re-emergence of the signals after introduction of the free acid form of the dye into the bathing solution. Note that the overall appearance of the cell and the Ca^{2+} signals before and after permeabilization are very similar. Figure 1*C* shows surface plots of Ca^{2+} sparks in intact and permeabilized cells in the presence of 0·1 or 0·5 mM EGTA. Table 1 summarizes spark statistics for the same conditions. As can be seen, permeabilization had no significant impact on the frequency, amplitude, width or length of the events (for all groups, $P > 0{\cdot}05$). The similarities in the spatio-temporal properties of Ca^{2+} sparks at 0·1 and 0·5 mM EGTA are likely to be due to the slow rate of Ca^{2+} binding by EGTA. The overall similarities between Ca^{2+} sparks and waves in intact and permeabilized cells suggest that our permeabilization procedure does not significantly alter the Ca^{2+} signalling mechanisms in the cell.

Effects of EGTA

Theoretical studies predict that soluble intracellular Ca^{2+} buffers must have a strong effect on interaction between release sites by lowering the rate of effective diffusion of Ca^{2+} (Keizer *et al.* 1998). We experimentally tested the effects of intracellular Ca^{2+} buffering on Ca^{2+} waves in

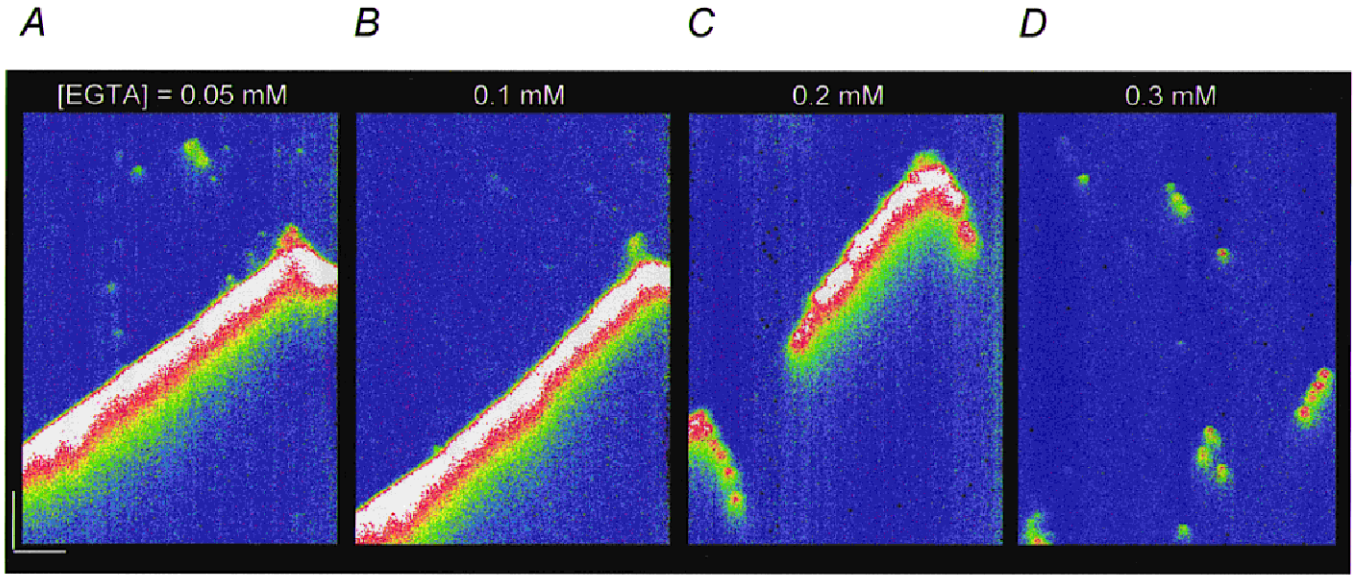

Figure 2. Effects of calcium buffering on Ca^{2+} waves in saponin-permeabilized myocytes

A, *B*, *C* and *D*, representative line-scan images of fluorescence recorded in a permeabilized myocyte in the presence of 0·05 mM (*A*), 0·1 mM (*B*), 0·2 mM (*C*) and 0·3 mM EGTA (*D*). Free [Ca^{2+}] in all cases was adjusted to 100 nM. Calibration bars: horizontal 15 μm, vertical 0·35 s.

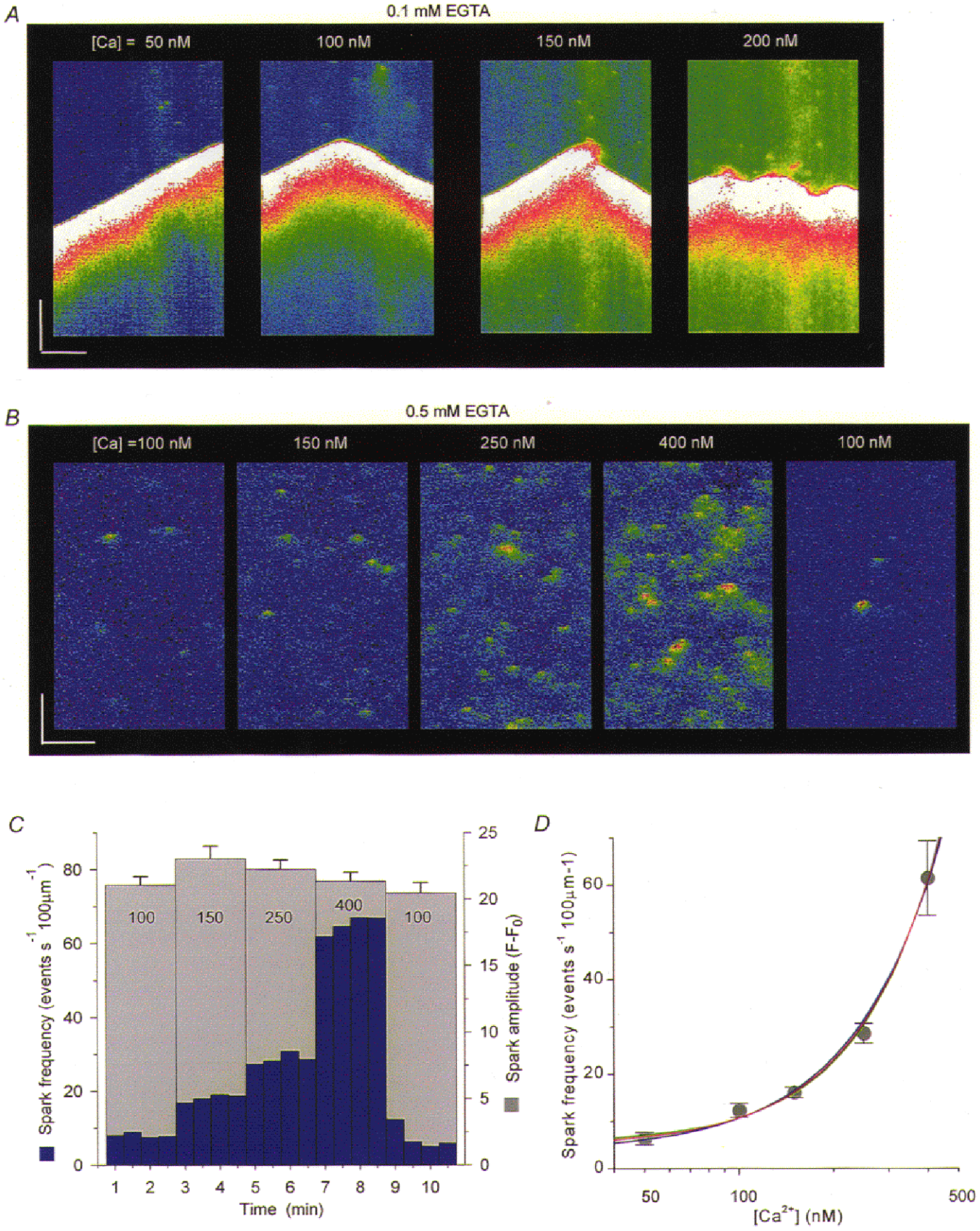

Figure 3. For legend see facing page.

Table 1. Spatio-temporal properties of Ca^{2+} sparks in intact and permeabilized ventricular cells

		Frequency[a]	Amplitude (F/F_o)	Duration (ms)[b]	Width (μm)[c]
Intact cells	$[Ca^{2+}]_o = 1$ mM	4·60 ± 0·48	1·69 ± 0·02	27·7 ± 1·1	1·75 ± 0·07
Skinned cells	[EGTA] = 0·1 mM	4·25 ± 0·88	1·72 ± 0·02	26·1 ± 0·7	1·85 ± 0·05
	[EGTA] = 0·5 mM	6·36 ± 0·65	1·71 ± 0·03	25·3 ± 0·6	1·96 ± 0·06

Data represented as means ± S.E.M. of measurements, $n = 30$–235. [a]Spark frequency was defined as the number of events per second per 100 μm line scanned. [b]Duration and [c]width of spark were measured at half-maximal amplitude.

permeabilized cardiac myocytes. In these experiments Ca^{2+} buffering strength was varied by addition of different concentrations of EGTA to the bathing solution, while adjusting basal Ca^{2+} to a constant value of 100 nM. In internal solutions with low Ca^{2+} buffering strength (0·05 mM EGTA), Ca^{2+} waves arose relatively frequently (0·06 ± 0·01 s^{-1}, $n = 21$) and propagated typically through the entire cell with a velocity of about 70 μm s^{-1} (66 ± 6 μm s^{-1}, $n = 21$; Fig. 2*A*). Elevation of EGTA concentration to 0·1 mM resulted in decreased frequency and propagation velocity of waves (0·03 ± 0·01 s^{-1} and 53 ± 1 μm s^{-1}, respectively, $n = 12$; Fig. 2*B*). Further increase in [EGTA] resulted in fragmentation of Ca^{2+} waves into abortive responses (Fig. 2*C* and *D*). Images obtained at high [EGTA] also clearly show that Ca^{2+} waves arise from sequential activation of discrete release events, revealing the saltatory nature of wave propagation. Propagating Ca^{2+} waves were completely abolished at [EGTA] > 0·3 mM. The fast Ca^{2+} buffer BAPTA prevented Ca^{2+} waves even at lower concentrations (~0·1 mM, not shown). These results indicate that Ca^{2+} buffering has a profound influence on Ca^{2+} waves.

Effects of $[Ca^{2+}]$

Ca^{2+} is the principal regulator of the activity of ryanodine receptors (RyRs) in the heart. Although the Ca^{2+} dependence of RyR activation and inactivation has been described in *in vitro* experiments (Coronado *et al.* 1994), the Ca^{2+} dependency of RyRs *in situ* remains uncertain because of the difficulties in measuring and controlling $[Ca^{2+}]$ in the diadic cleft during E–C coupling. We took advantage of our permeabilized myocyte preparation to investigate the relationship between Ca^{2+} and the activity of Ca^{2+} release sites. Figure 3*A* illustrates the effects of increasing $[Ca^{2+}]$ from 50 nM to 100, 150 or 200 nM in the presence of 0·1 mM EGTA. Elevating $[Ca^{2+}]$ resulted in increased frequency of Ca^{2+} waves. In addition, at elevated $[Ca^{2+}]$ multi-focal Ca^{2+} waves arising simultaneously from several independent sites became evident. Quantitative assessments of spark properties at high $[Ca^{2+}]$ were impaired by the presence of Ca^{2+} waves and elevated background fluorescence. Increases in background fluorescence also limited the Ca^{2+} concentrations in the experimental solution to a rather limited range because of saturation of the photomultiplier at high $[Ca^{2+}]_i$. Therefore, we employed bathing solutions containing high [EGTA] to abolish spontaneous Ca^{2+} waves. We also corrected the images for changes in background fluorescence at different $[Ca^{2+}]_i$ by adjusting the fluorescence of the bathing solution outside the permeabilized cells to the same level. Figure 3*B* shows representative images from such an experiment recorded during successive increases of $[Ca^{2+}]$ from 100 to 150, 250 and 400 nM and a subsequent return

Figure 3. Effects of $[Ca^{2+}]_i$ on Ca^{2+} sparks and Ca^{2+} waves in saponin-permeabilized myocytes

A, representative line-scan images of fluorescence recorded in a permeabilized myocyte at various $[Ca^{2+}]_i$ levels (indicated at the top of the respective images) in the presence of 0·1 mM EGTA. *B*, line-scan images of Ca^{2+} sparks corrected for increases of background fluorescence at various $[Ca^{2+}]_i$ levels (indicated at the top of the respective images) in the presence of 0·5 mM EGTA. Calibration bars: horizontal 15 μm (*A*) and 20 μm (*B*), vertical 0·5 s (*A*) and 0·1 s (*B*). *C*, Ca^{2+} spark frequency (blue) and amplitude (light grey) as a function of time before and after elevating $[Ca^{2+}]_i$ to indicated levels for the experiment shown in *B*. *D*, Ca^{2+} spark frequency as a function of $[Ca^{2+}]_i$. The values are represented as means ± S.E.M. obtained in 5 experiments. The lines were obtained by fitting the data according to the equation $f = f_{max}\{[Ca^{2+}]^n/([Ca^{2+}]^n + K_D{}^n)\}$, where $f_{max} = 10\,000$ events s^{-1} $(100\ \mu m)^{-1}$, $K_D = 9{\cdot}9\ \mu M$ and $n = 1{\cdot}6$ (blue line); $f_{max} = 20\,000$ events s^{-1} $(100\ \mu m)^{-1}$; $K_D = 15\ \mu M$ and $n = 1{\cdot}6$ (red line); and $f_{max} = 30\,000$ events s^{-1} $(100\ \mu m)^{-1}$; $K_D = 20\ \mu M$ and $n = 1{\cdot}6$ (green line).

Table 2. Spatio-temporal properties of Ca^{2+} sparks in permeabilized ventricular cells before and after addition of calmodulin or cADPR

		Frequency[a]	Amplitude (F/F_o)	Duration (ms)[b]	Width (μm)[c]
[Calmodulin]	0	7·7 ± 1·2	1·8 ± 0·02	26 ± 0·9	2·02 ± 0·06
	5 μM	15·5 ± 2·2*	1·9 ± 0·03	27 ± 0·6	1·93 ± 0·04
[cADPR]	0	5·1 ± 1·1	1·5 ± 0·02	29 ± 1·4	1·92 ± 0·11
	5 μM	8·9 ± 1·8*	1·5 ± 0·01	29 ± 1·3	1·94 ± 0·09

Data represented as means ± S.E.M. of measurements, $n = 24$–329. [a]Spark frequency was defined as the number of events per second per 100 μm line scanned. [b]Duration and [c]width of spark were measured at half-maximal amplitude. *Significantly different from control at $P < 0·05$.

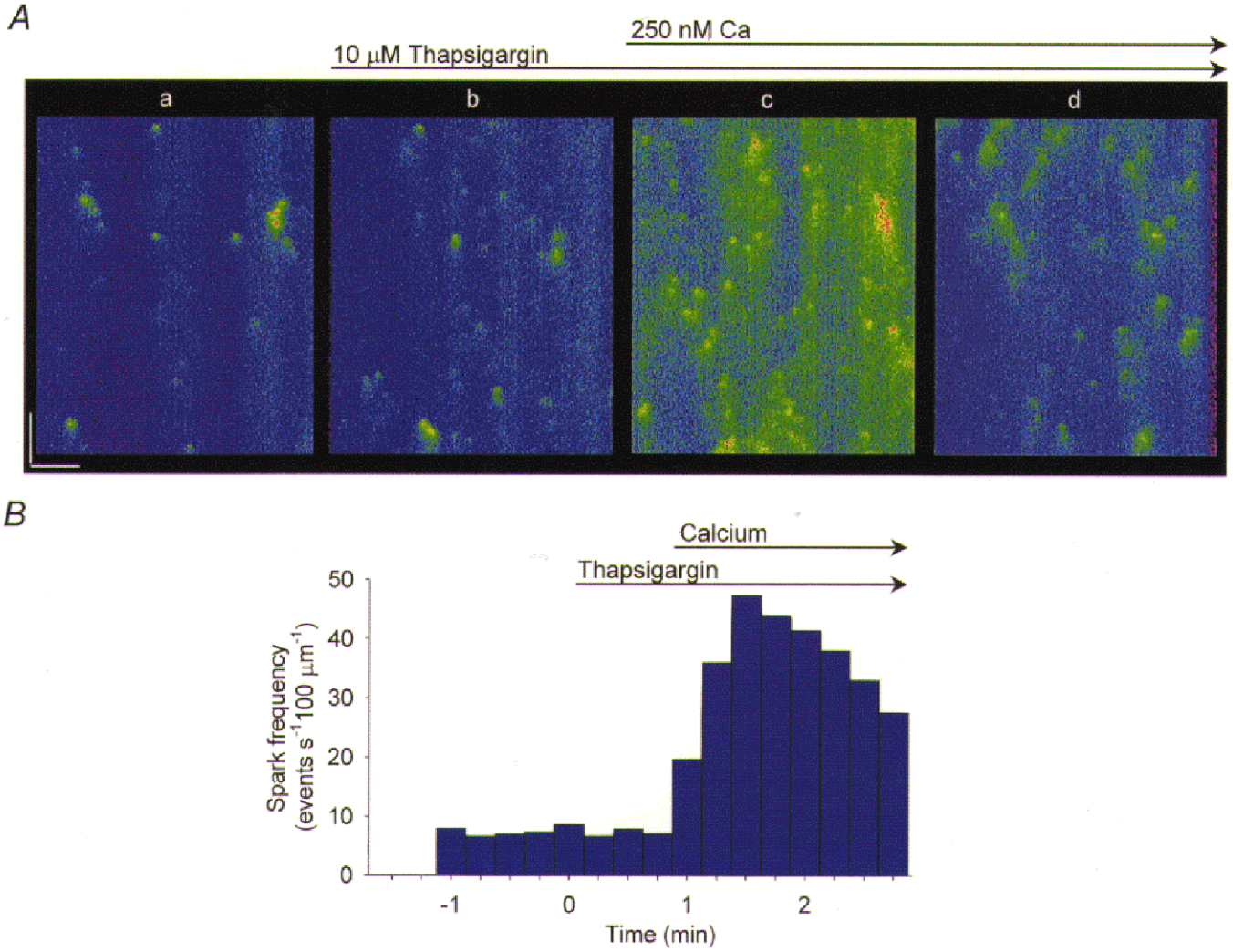

Figure 4. The effects of elevating $[Ca^{2+}]_i$ on sparking activity in the presence of thapsigargin

A, representative line-scan images of fluorescence acquired before (*a* and *b*) and at different times (2 and 3 min) after increasing $[Ca^{2+}]_i$ from 80 nM to 250 nM in the presence of thapsigargin (*c* and *d*, respectively). Thapsigargin (10 μM) was introduced into the bathing solution 1 min before elevating $[Ca^{2+}]_i$. Calibration bars: horizontal 20 μm, vertical 0·15 s. *B*, Ca^{2+} spark frequency as a function of time before and after the addition of thapsigargin into the bathing solution in the same experiment. The experimental protocol is presented schematically at the top.

to 100 nM. The effects of $[Ca^{2+}]$ on the frequency and amplitude of Ca^{2+} sparks from the same experiment are documented in Fig. 3*C*. Increasing $[Ca^{2+}]$ in the range 100–400 nM resulted in a gradual increase in frequency of sparks. Changing back to the original solution with 100 nM Ca^{2+} resulted in restoration of spark frequency to the control level, thus indicating no significant signs of a run-down in sparking activity. The changes in the frequency of sparks were accompanied only by insignificant alterations in the amplitude of sparks (10 % at 150 nM $[Ca^{2+}]$, grey bars). The results of five experiments are summarized in Fig. 3*D*, which plots the frequency of Ca^{2+} sparks as a function of $[Ca^{2+}]$. It is unlikely that the amplitude of Ca^{2+} sparks was saturated at elevated $[Ca^{2+}]$. The K_D of fluo-3 in the myoplasm has been estimated to be near 1 μM (Harkins *et al.* 1993). Ca^{2+} sparks with an amplitude of 200–300 nM would rise above a background $[Ca^{2+}]$ of 400 nM only to a level of 600–700 nM, which still would be in the linear range of the indicator.

The observed potentiation of Ca^{2+} sparks could be attributed also to a possible increase in the SR Ca^{2+} content (Fabiato, 1992; Orchard *et al.* 1998) affecting the activity of the Ca^{2+} release channels at luminal sites (Györke & Györke, 1998). We assessed the potential role of this mechanism, by using thapsigargin to prevent accumulation of extra Ca^{2+} into the SR upon elevation of cytosolic Ca^{2+}. Representative images from such an experiment are shown in Fig. 4*A*. The effects of $[Ca^{2+}]$ on spark frequency in the same experiment are quantified in Fig. 4*B*. We applied 10 μM thapsigargin for 1 min before elevating $[Ca^{2+}]$ from 100 nM to 250 nM. At this concentration and exposure time thapsigargin inhibits SR Ca^{2+} uptake without causing a significant loss in the SR Ca^{2+} content (Bassani *et al.* 1993; Lukyanenko *et al.* 1999). Under these experimental conditions increasing $[Ca^{2+}]_i$ resulted in an about 6-fold (from $7{\cdot}1 \pm 0{\cdot}9$ to $39{\cdot}8 \pm 1{\cdot}9$ event s^{-1} $(100\ \mu m)^{-1}$, $n = 5$) increase in sparking frequency, which is similar to that observed in experiments without thapsigargin. Following more than 2–3 min of continuous exposure to thapsigargin, the frequency of sparks gradually decreased, apparently due to a loss of Ca^{2+} from the SR (Bassani *et al.* 1993; Lukyanenko *et al.* 1999). Taken together, these results suggest that under our experimental conditions, the increase in sparking activity cannot be attributed to increased SR Ca^{2+} load.

Effects of calmodulin and cADPR

We tested the effects on release site activity of certain membrane-impermeable putative regulators of the SR Ca^{2+} release such as cyclic adenosine diphosphate-ribose (cADPR, MW 541·3) and calmodulin (MW 16 680), which would be difficult to study in cells with an intact sarcolemma. Figure 5 illustrates representative images of Ca^{2+} sparks before and after exposure of two permeabilized cells to calmodulin (*A*, 5 μM) and cADPR (*C*, 5 μM), while Table 2 summarizes the effects of these drugs on Ca^{2+} spark properties. Both drugs caused dramatic increases in the frequency of Ca^{2+} sparks with no significant changes in the amplitude and spatio-temporal properties of the events. The effects of cADPR developed over a period of 2–6 min, and they were readily reversible. The onset of potentiation of Ca^{2+} sparks by calmodulin was considerably slower, 10–15 min. In addition, the cells showed no significant recovery upon reverting to the control solution during a period of 5–10 min. The slow onset and lack of reversibility of calmodulin effects could be attributed to the slow diffusion rate of this high molecular weight agent as well as to the fact that the effects are likely to involve long-lasting biochemical changes (phosphorylation of SR proteins). Incubation of the cells with calmodulin also resulted in a significant increase in the amplitude of caffeine-induced Ca^{2+} transients ($31{\cdot}2 \pm 4{\cdot}4$ %, $n = 5$; Fig. 5*B*), suggesting that the effects of this agent on Ca^{2+} sparks might be mediated by changes in the SR Ca^{2+} load. These results further illustrate our ability to manipulate the environment of the release sites in ways not possible in intact cells.

DISCUSSION

In the present study we investigated the Ca^{2+}-releasing activity of the SR in saponin-permeabilized cardiac myocytes using confocal Ca^{2+} imaging. In essential internal solutions designed to maintain the basic functional integrity of Ca^{2+} stores, permeabilized cardiac myocytes exhibited Ca^{2+} sparks and Ca^{2+} waves similar to those observed in intact cells. During permeabilization, the content of the cells is diluted in the internal bathing solution (~100 000-fold dilution). Thus, it appears that no endogenous factors such as cytosolic kinases and phosphatases that could be lost through equilibration with the bathing solution are essential to maintaining basic activation and inactivation properties of the release sites.

We described explicitly the dependency of spark frequency upon $[Ca^{2+}]$ in the range 50–400 nM. It is interesting to speculate how these results might relate to the overall Ca^{2+} dependency of Ca^{2+} spark activation in cardiomyocytes. If we assume that all of the the approximately 200 release units (Sommer, 1995; Franzini-Armstrong & Protasi, 1997) contained in the volume of a rectangular block of approximately 1 μm width (diameter of the laser beam spot), 1 μm height (depth of field of the microscope) and 100 μm length scanned along a myocyte can be activated within 10 ms (Cannell *et al.* 1994), the maximal frequency of sparks would be 20 000 events s^{-1} $(100\ \mu m)^{-1}$. This maximal sparking rate would be consistent with the estimated frequency of sparks during action potential stimulation, when presumably most of the release units become activated (~15 000 events s^{-1} $(100\ \mu m)^{-1}$, Cannel *et al.* 1994). We fitted our data presented in Fig. 3*D* to Hill functions with three different maximal sparking rates of 10 000, 20 000 and 30 000 events s^{-1} $(100\ \mu m)^{-1}$ (Fig. 3*D*). The best fits to the data for the three specified maximal sparking rates yielded Ca^{2+} dissociation constants of 9·9, 15·2 and

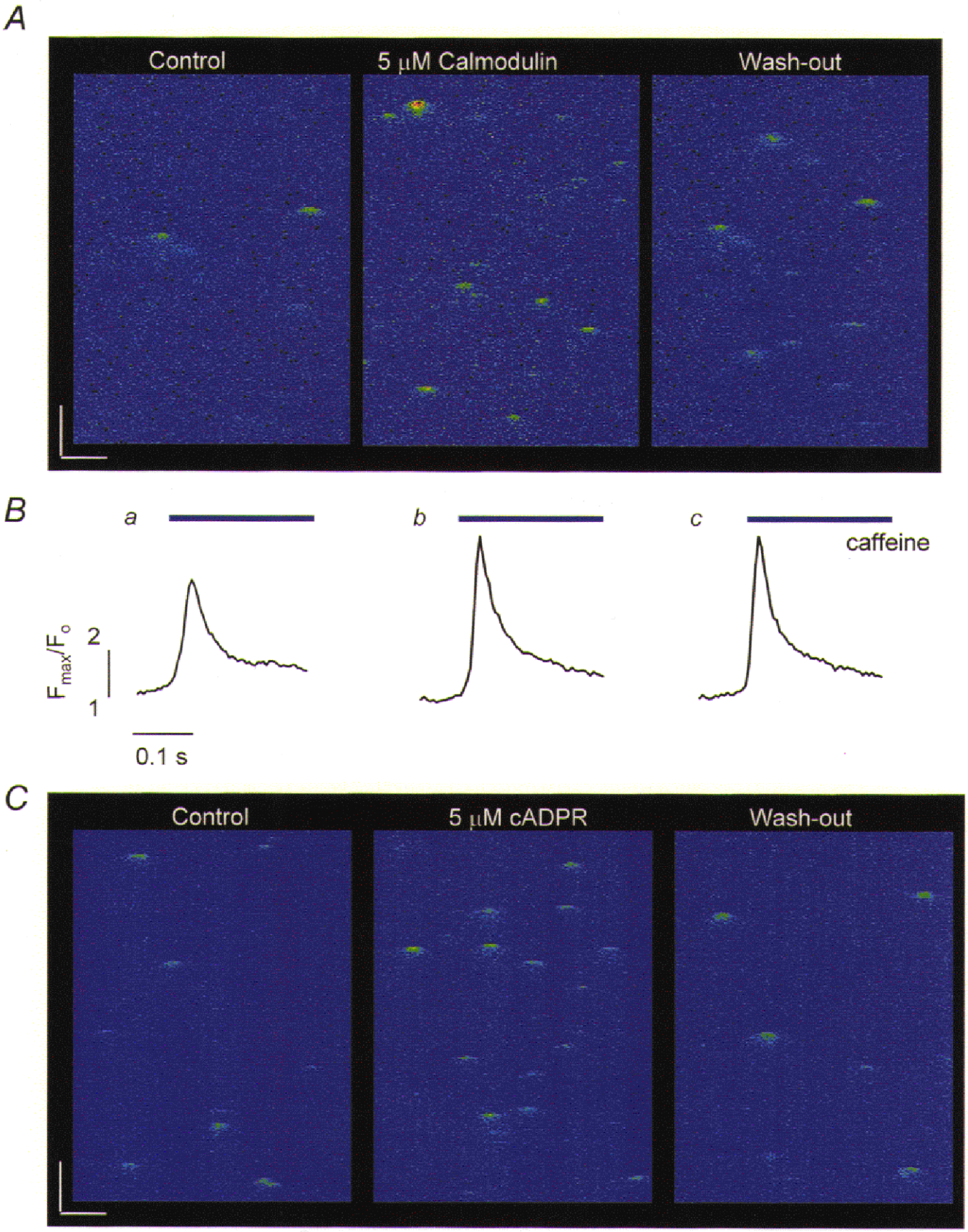

Figure 5. For legend see facing page.

19·6 μM and Hill coefficients equal to 1·6 in all cases. The estimated values of K_D of Ca^{2+} sensitivity of release sites are in the range of Ca^{2+} dependency of RyR open probability measured in lipid bilayer experiments in the presence of physiological concentrations of Mg^{2+} and ATP ($K_D \approx 30$ μM; Györke & Györke, 1998). The relatively low K_D and supra-linear dependency of release site activation on [Ca^{2+}] could explain why most release events normally remain localized and do not initiate calcium-induced calcium release (CICR) in the neighbouring release sites (Stern *et al.* 1999). We should point out, however, that because of the limited range of [Ca^{2+}] over which the sparks could be measured the obtained characteristics of Ca^{2+} dependency of release sites represent only approximate estimates.

In mechanically skinned Purkinje cells, Fabiato showed that sub-micromolar basal Ca^{2+} resulted in a substantial decrease in the macroscopic CICR, suggesting that Ca^{2+} release is inhibited at a high affinity inactivation site (Fabiato, 1985). Under our experimental conditions, sparking activity does not appear to be influenced by such a high Ca^{2+} affinity inactivation process because spark frequency only increased steadily upon elevations of [Ca^{2+}]. Our results, however, do not rule out the possibility that local release events are controlled by high local Ca^{2+} through a low-affinity inactivation process. Inhibition of RyRs by Ca^{2+} in a range of 50 μM to 10 mM has been reported in both lipid bilayer (Laver *et al.* 1995; Copello *et al.* 1997; Györke & Györke, 1988; Marengo *et al.* 1998) and vesicle flux experiments (Chamberlain *et al.* 1984; Zimanyi & Pessah, 1991; Chu *et al.* 1993). Such a low affinity inactivation, as well as a possible use-dependent inactivation induced by prior activation of the channel (Sham *et al.* 1998; Zahradnikova *et al.* 1999), could contribute to local release termination without influencing the stationary frequency of sparks. Indeed, at the sub-micromolar [Ca^{2+}] employed in our experiments, the probability of reactivation of individual release units must be quite low ($P = 0·09$ assuming 200 independent release units sparking at a rate of 60 events s^{-1} (100 $\mu m)^{-1}$) for time periods compatible with the time of recovery from such inactivated conditions (~1 s).

The propagating Ca^{2+} waves were profoundly influenced by Ca^{2+} buffering. At low Ca^{2+} buffering strength (EGTA < 100 μM), waves arose regularly even at low [Ca^{2+}]. Increasing EGTA resulted in decreased wave generation. Propagating Ca^{2+} waves were completely abolished at EGTA > 0·3 mM. These results reveal the importance of intracellular Ca^{2+} buffering in the confinement of CICR in cardiac cells. The high sensitivity of Ca^{2+} wave propagation to Ca^{2+} buffering is consistent with a saltatory mechanism of Ca^{2+} wave propagation (Keizer *et al.* 1998; Lukyanenko *et al.* 1999). In contrast to a continuous model of Ca^{2+} waves in a saltatory model, the release sites are spatially separated and thus are sensitive to interventions impairing the free diffusion of Ca^{2+}. In fact, site-to-site propagation by sequential activation of Ca^{2+} sparks was evident in the presence of intermediate EGTA concentrations (Fig. 2*C* and *D*).

The activity of release sites was affected by the endogenous signalling molecules calmodulin and cADPR. Interestingly, calmodulin, which has been shown to inhibit RyRs (by direct interaction or through the activation of Ca^{2+}–calmodulin-dependent protein kinase) in most RyR reconstitution studies (Meissner & Henderson, 1987; Takasago *et al.* 1991; Lokuta *et al.* 1995; Hain *et al.* 1995), enhanced sparking activity in cardiac cells. We attribute this potentiation to increased accumulation of Ca^{2+} within the SR due to stimulation of the SR Ca^{2+}-ATPase (Narayanan & Xu, 1997) and subsequent activation of RyRs by Ca^{2+} at luminal sites (Györke & Györke, 1988). Indeed, exposure of the cells to calmodulin resulted in a significant increase in the SR Ca^{2+} content (Fig. 5*B*). These results are in line with the previous studies suggesting that luminal Ca^{2+} is a critical determinant of the functional state of Ca^{2+} release in cardiac muscle (Bassani *et al.* 1995; Györke *et al.* 1997; Eisner *et al.* 1998). The demonstrated potentiation of Ca^{2+} sparks by cADPR supports the previous studies suggesting that cADPR can enhance Ca^{2+} release presumably through potentiation of RyRs (Meszaros *et al.* 1993; Iino *et al.* 1997; Galione *et al.* 1998). Taken together, our results show that saponin-permeabilized cells can be a useful model system for studying both spatial and temporal aspects of Ca^{2+} signalling in the heart under conditions in which the environment surrounding the Ca^{2+} release channels can be controlled precisely.

Figure 5. Effects of calmodulin and cADPR on Ca^{2+} sparks

A, representative line-scan images of fluorescence changes acquired under control conditions (left-hand panel), 15 min after exposure of the cells to 5 μM calmodulin (middle panel), and 10 min after changing back to the control solution (right-hand panel). Calibration bars: horizontal 10 μm, vertical 0·2 s. *B*, caffeine-induced Ca^{2+} transients measured in the same cell at the same stages of the experiment as in *A*. Caffeine (20 mM) was applied for 2 s. *C*, representative line-scan images of fluorescence changes measured under control conditions (left-hand panel), 2 min after exposure of the cells to 5 μM cADPR (middle panel), and 5 min after reverting back to the control solution (right-hand panel). Calibration bars: horizontal 10 μm, vertical 0·2 s.

Bassani, J. W., Bassani, R. A. & Bers, D. M. (1993). Twitch-dependent SR Ca accumulation and release in rabbit ventricular myocytes. *American Journal of Physiology* **265**, C533–540.

Bassani, J. W., Yuan, W. & Bers, D. M. (1995). Fractional SR Ca^{2+} release is regulated by trigger Ca^{2+} and SR Ca^{2+} content in cardiac myocytes. *American Journal of Physiology* **268**, C1313–1329.

Bers, D. M. (1991). *Excitation–Contraction Coupling and Cardiac Contractile Force*. Kluwer Academic Publishers, Dordrecht, The Netherlands.

Cannell, M. B., Cheng, H. & Lederer, W. J. (1994). Spatial non-uniformities in $[Ca^{2+}]_i$ during excitation–contraction coupling in cardiac myocytes. *Biophysical Journal* **67**, 1942–1956.

Chamberlain, B. K., Volpe, P. & Fleischer, S. (1984). Calcium-induced calcium release from purified cardiac sarcoplasmic reticulum vesicles. *Journal of Biological Chemistry* **259**, 7540–7546.

Cheng, H., Lederer, W. & Cannell, M. B. (1993). Calcium sparks: elementary events underlying excitation–contraction coupling in heart muscle. *Science* **262**, 740–744.

Cheng, H., Lederer, M. R., Lederer, W. J. & Cannell, M. B. (1996). Calcium sparks and $[Ca^{2+}]_i$ waves in cardiac myocytes. *American Journal of Physiology* **270**, C148–159.

Cheng, H., Song, L. S., Shirokova, N., Gonzalez, A., Lakatta, E. G., Rios, E. & Stern, M. D. (1999). Amplitude distribution of calcium sparks in confocal images: theory and studies with an automatic detection method. *Biophysical Journal* **76**, 606–617.

Chu, A., Fill, M., Stefani, E. & Entman, M. L. (1993). Cytoplasmic Ca^{2+} does not inhibit the cardiac muscle sarcoplasmic reticulum ryanodine receptor Ca^{2+} channel, although Ca^{2+}-induced Ca^{2+} inactivation of Ca^{2+} release is observed in native vesicles. *Journal of Membrane Biology* **135**, 49–59.

Copello, J. A., Barg, S., Onoue, H. & Fleicher, S. (1997). Heterogeneity of Ca^{2+} gating of skeletal muscle and cardiac ryanodine receptor. *Biophysical Journal* **73**, 141–156.

Coronado, R., Morrissette, J., Sukhareva, M. & Vaughan, D. M. (1994). Structure and function of ryanodine receptors. *American Journal of Physiology* **266**, C1485–1504.

Eisner, D. A., Trafford, A. W., Diaz, M. E., Overend, C. L. & O'Neill, S. C. (1998). The control of Ca release from the cardiac sarcoplasmic reticulum: regulation *versus* autoregulation. *Cardiovascular Research* **38**, 589–604.

Engel, J., Sowerby, A. J., Finch, A. E., Fechner, M. & Stier, A. (1995). Temperature dependence of Ca^{2+} wave properties in cardiomyocytes: implications for the mechanism of autocatalytic Ca^{2+} release in wave propagation. *Biophysical Journal* **68**, 40–45.

Fabiato, A. (1985). Time and calcium dependence of activation and inactivation of calcium-induced calcium release of calcium from the sarcoplasmic reticulum of a skinned canine cardiac Purkinje cell. *Journal of General Physiology* **85**, 291–320.

Fabiato, A. (1992). Two kinds of calcium-induced release of calcium from the sarcoplasmic reticulum of skinned cardiac cells. In *Excitation–Contraction Coupling in Skeletal, Cardiac and Smooth Muscle*, ed. Frank, G. B., pp. 245–262. Plenum Press, New York.

Franzini-Armstrong, C. & Protasi, F. (1997). Ryanodine receptors of striated muscles: a complex channel capable of multiple interactions. *Physiological Reviews* **77**, 699–729.

Galione, A., Cui, Y., Empson, R., Iino, S., Wilson, H. & Terrar, D. (1998). Cyclic ADP-ribose and the regulation of calcium-induced calcium release in eggs and cardiac myocytes. *Cell Biochemistry and Biophysics* **28**, 19–30.

Györke, I. & Györke, S. (1998). Regulation of the cardiac ryanodine receptor channel by luminal Ca^{2+} involves luminal Ca^{2+} sensing sites. *Biophysical Journal* **75**, 2801–2810.

Györke, S., Lukyanenko, V. & Györke, I. (1997). Dual effects of tetracaine on spontaneous calcium release in rat ventricular myocytes. *Journal of Physiology* **500**, 297–309.

Hain, J., Onoue, H., Mayrleitner, M., Fleischer, S. & Schindler, H. (1995). Phosphorylation modulates the function of the calcium release channel of sarcoplasmic reticulum from cardiac muscle. *Journal of Biological Chemistry* **270**, 2074–2081.

Harkins, A. B., Kurebayashi, N. & Baylor, S. M. (1993). Resting myoplasmic free calcium in frog skeletal muscle fibers estimated with fluo-3. *Biophysical Journal* **65**, 865–881.

Iino, S., Cui, Y., Galione, A. & Terrar, D. A. (1997). Actions of cADP-ribose and its antagonists on contraction in guinea pig isolated ventricular myocytes. Influence of temperature. *Circulation Research* **81**, 879–884.

Ishide, N. (1996). Intracellular calcium modulators for cardiac muscle in pathological conditions. *Japanese Heart Journal* **37**, 1–17.

Keizer, J., Smith, G., Ponce-Dawson, S. & Pearson, J. (1998). Saltatory propagation of Ca^{2+} waves by Ca^{2+} sparks. *Biophysical Journal* **75**, 595–600.

Kort, A. A., Capogrossi, M. C. & Lakatta, E. G. (1985). Frequency, amplitude, and propagation velocity of spontaneous Ca^{2+}-dependent contractile waves in intact adult rat cardiac muscle and isolated myocytes. *Circulation Research* **57**, 844–855.

Lakatta, E. G. (1992). Functional implications of spontaneous sarcoplasmic reticulum Ca^{2+} release in the heart. *Cardiovascular Research* **26**, 193–214.

Laver, D. R., Roden, L. D., Ahern, G. P., Eager, K. R., Junankar, P. R. & Dulhunty, A. F. (1995). Cytoplasmic Ca^{2+} inhibits the ryanodine receptor from cardiac muscle. *Journal of Membrane Biology* **147**, 7–22.

Lipp, P. & Niggli, E. (1994). Modulation of Ca^{2+} release in cultured neonatal rat cardiac myocytes. *Circulation Research* **74**, 979–990.

Lokuta, A. J., Rogers, T. B., Lederer, W. J. & Valdivia, H. H. (1995). Modulation of cardiac ryanodine receptors of swine and rabbit by a phosphorylation-dephosphorylation mechanism. *Journal of Physiology* **487**, 609–622.

Lopez-Lopez, J. R., Shacklock, P. S., Balke, C. W. & Wier, W. G. (1995). Local calcium transients triggered by single L-type calcium channel currents in cardiac cells. *Science* **268**, 1042–1045.

Lukyanenko, V., Györke, I. & Györke, S. (1996). Regulation of calcium release by calcium inside the sarcoplasmic reticulum in ventricular myocytes. *Pflügers Archiv* **432**, 1047–1054.

Lukyanenko, V., Subramanian, S., Györke, I., Wiesner, T. & Györke, S. (1999). The role of luminal Ca^{2+} in generation of Ca^{2+} waves in rat ventricular myocytes. *Journal of Physiology* **518**, 173–186.

Marengo, J. J., Hidalgo, C. & Bull, R. (1998). Sulfhydryl oxidation modifies the calcium dependence of ryanodine-sensitive calcium channels of excitable cells. *Biophysical Journal* **74**, 1263–1277.

Meissner, G. & Henderson, J. S. (1987). Rapid calcium release from cardiac sarcoplasmic reticulum vesicles is dependent on Ca^{2+} and is modulated by Mg^{2+}, adenine nucleotide, and calmodulin. *Journal of Biological Chemistry* **262**, 3065–3073.

Meszaros, L. G., Bak, J. & Chu, A. (1993). Cyclic ADP-ribose as an endogenous regulator of the non-skeletal type ryanodine receptor Ca^{2+} channel. *Nature* **364**, 76–79.

Narayanan, N. & Xu, A. (1997). Phosphorylation and regulation of the Ca(2+)-pumping ATPase in cardiac sarcoplasmic reticulum by calcium/calmodulin-dependent protein kinase. *Basic Research in Cardiology* **92** (suppl. 1), 25–35.

Orchard, C. H., Smith, G. L. & Steele, D. S. (1998). Effects of cytosolic Ca^{2+} on the Ca^{2+} content of the sarcoplasmic reticulum in saponin-permeabilized rat ventricular trabeculae. *Pflügers Archiv* **435**, 555–563.

Sham, J. S., Song, L. S., Chen, Y., Deng, L. H., Stern, M. D., Lakatta, E. G. & Cheng, H. (1998). Termination of Ca^{2+} release by a local inactivation of ryanodine receptors in cardiac myocytes. *Proceedings of the National Academy of Sciences of the USA* **95**, 15096–15101.

Sommer, J. R. (1995). Comparative anatomy: in praise of a powerful approach to elucidate mechanisms translating cardiac excitation into purposeful contraction. *Journal of Molecular Cell Cardiology* **27**, 19–35.

Song, L. S., Stern, M. D., Lakatta, E. G. & Cheng, H. (1997). Partial depletion of sarcoplasmic reticulum calcium does not prevent calcium sparks in rat ventricular myocytes. *Journal of Physiology* **505**, 665–675.

Stern, M. D. & Lakatta, E. (1992). Excitation–contraction in the heart: the state of the question. *FASEB Journal* **6**, 3092–3100.

Stern, M. D., Song, L. S., Cheng, H., Sham, J. S., Yang, H. T., Boheler, K. R. & Rios, E. (1999). Local control models of cardiac excitation–contraction coupling. A possible role for allosteric interactions between ryanodine receptors. *Journal of General Physiology* **113**, 469–489.

Sitsapesan, R. & Williams, A. J. (1995). Cyclic ADP-ribose and related compounds activate sheep skeletal sarcoplasmic reticulum Ca^{2+} release channel. *American Journal of Physiology* **268**, C1235–1240.

Takamatsu, T. & Wier, W. G. (1990). Calcium waves in mammalian heart: quantification of origin, magnitude, waveform, and velocity. *FASEB Journal* **4**, 1519–1525.

Takasago, T., Imagawa, T., Furukawa, K., Ogurusu, T. & Shigekawa, M. (1991). Regulation of the cardiac ryanodine receptor by protein kinase-dependent phosphorylation. *Journal of Biochemistry* (Tokyo) **109**, 163–170.

Trafford, A. W., Lipp, P., O'Neil, C. O., Niggli, E. & Eisner, D. A. (1995). Propagating calcium waves initiated by local caffeine application in rat ventricular myocytes. *Journal of Physiology* **489**, 319–326.

Wier, W. G., Cannell, M. B., Berlin, J. R., Marban, E. & Lederer, W. J. (1987). Cellular and subcellular heterogeneity of $[Ca^{2+}]_i$ in single heart cells revealed by Fura-2. *Science* **235**, 325–328.

Wussling, M. H. & Salz, H. (1996). Nonlinear propagation of spherical calcium waves in rat cardiac myocytes. *Biophysical Journal* **70**, 1144–1153.

Zahradníková, A., Dura, M. & Györke, S. (1999). Modal gating transitions in cardiac ryanodine receptors during increases of Ca^{2+} concentration produced by photolysis of caged Ca^{2+}. *Pflügers Archiv* **438**, 283–288.

Zimanyi, I. & Pessah, I. N. (1991). Comparison of [^{3}H]ryanodine receptors and Ca^{2+} release from rat cardiac and rabbit skeletal muscle sarcoplasmic reticulum. *Journal of Pharmacology and Experimental Therapeutics* **256**, 938–946.

Acknowledgements

This work was supported by the National Institutes of Health (HL 63043, HL 52620, HL 03739). S. Györke is an Established Investigator of the American Heart Association.

Corresponding author

S. Györke: Department of Physiology, Texas Tech University HSC, Lubbock, TX 79430, USA.